Precise glass temperatures

2003 J. Phys.: Condens. Matter 15 S789

(http://iopscience.iop.org/0953-8984/15/11/304)

INSTITUTE OF PHYSICS PUBLISHING JOURNAL OF PHYSICS: CONDENSED MATTER

J. Phys.: Condens. Matter **15** (2003) S789–S802 PII: S0953-8984(03)58065-1

Precise glass temperatures

Donald J Plazek and Craig A Bero[1]

University of Pittsburgh, Pittsburgh, PA 15261, USA

Received 27 September 2002
Published 10 March 2003
Online at stacks.iop.org/JPhysCM/15/S789

Abstract

Since the glass temperature T_g is a corresponding temperature for amorphous materials, if measured properly, precise values are needed. When determinations are made by cooling from equilibrium, material characterizing values are obtained. Most reported values are obtained in heating experiments which yield specimen-specific values, which approximate fictive temperatures T_f. Examples of consequent discrepancies of relaxation times at T_g are given. Results obtained in cooling show that it is likely that the mobility at T_g of local molecular motions is the same for all of the amorphous materials examined. In addition, it is shown that relatively precise values of T_g can be obtained from the recoverable compliance.

1. Introduction

It is virtually universally accepted that at the glass temperature T_g of a liquid, due to molecular crowding with a consequent decrease in molecular mobility, the molecular rearrangement of the liquid structure can no longer keep up with the applied rate of cooling and equilibrium is lost. Upon further cooling the specific volume and enthalpy have values that are greater than their equilibrium or metastable equilibrium values (Kovacs 1964). Note that it is the lack of maintaining equilibrium that is involved. No transition occurs and the term 'glass transition' is a misnomer.

It follows that, if the glass temperature is to be a material characterizing parameter, it must be determined as a function of the rate in a cooling experiment (Plazek and Ngai 1996). The material must start out in equilibrium. However, most reported values have been estimated in heating experiments. By standardizing the preceding cooling history followed by heating immediately after reaching the lowest temperature, so as to minimize physical ageing, T_g can be approximated (Richardson and Savill 1975, DeBolt *et al* 1976, Plazek and Frund 1990). Most measurements have been made utilizing differential scanning calorimeters, DSC, because of their convenience. In the past, calibrating the temperature scale in cooling has been possible only with monumental difficulty because of the supercooling of melting point standards (Richardson and Savill 1977). However, liquid crystal spinodal decompositions do

[1] Present address: MSA, Cranberry Twp., PA 16066, USA.

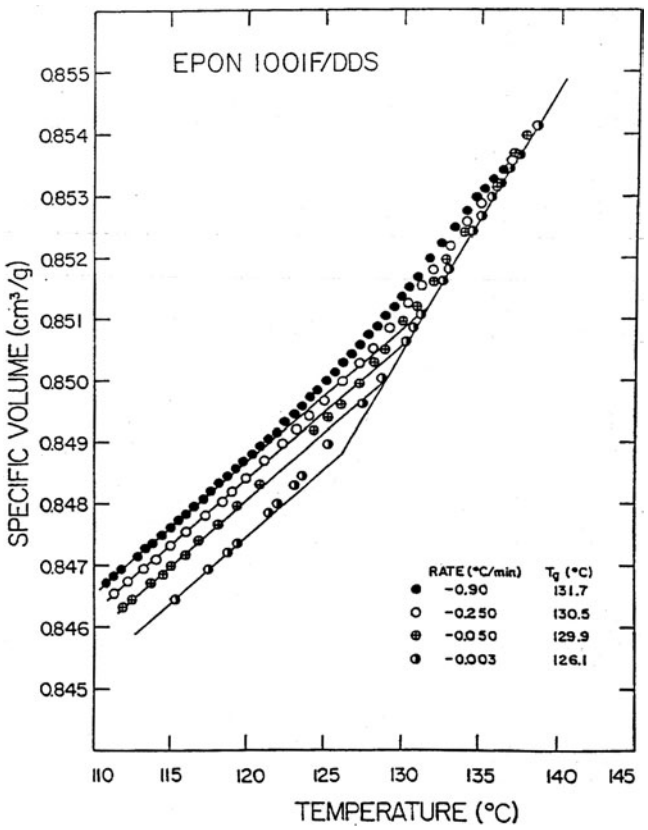

Figure 1. The specific volume V (cm^3 g^{-1}) of an epoxy resin Epon 1001F, fully cured with a stoichiometric amount of DDS, shown as a function of temperature at four rates of cooling, as indicated. Glass temperatures are identified by the intersection points of the equilibrium and glass lines.

not supercool, so temperature calibration during cooling is now possible. The smectic-to-cholesteric transition of (+)-4-n-hexyloxyphenyl-4′-(2′-methyl butyl)-biphenyl-4-carboxylate at 78.8 °C is one such transition (CE-3 from T M Leslie, University of Alabama).

Among the most dependable determinations of T_g are those carried out in dilatometric cooling experiments. They are more laborious than DSC determinations and are not as sophisticated as multidimensional NMR, atomic force microscopy, or back-scattered neutron studies; and, OSHA (the US Occupational Safety and Health Administration) forbid, mercury is the usual containing liquid. Greiner and Schwarzl have given us the most exhaustive dilatometric results on four polymers, polystyrene (PS), polyvinyl chloride (PVC), polymethyl methacrylate (PMMA), and polycarbonate (PC), including the T_g-dependence on the rate of cooling (Greiner and Schwarzl 1984). We have contributed similar data on an epoxy resin Epon 1001, fully cured with a stoichiometric amount of 4, 4′-diaminodiphenyl sulfone, DDS (Bero and Plazek 1991). Epon 1001 is a diglycidyl ether of bisphenol A, described by LeMay *et al* (see figure 1). The number of dependable T_gs is we believe quite small and we wish to illustrate some of the consequences of the lack of attention paid to this important characterizing parameter. Like the weather, it is much discussed but not pursued.

However, it must be acknowledged that a multifaceted approach is necessary in the investigation of glassy behaviour; as Bohmer *et al* in a recent extensive review on the ‘Dynamics

of supercooled liquids and glassy solids' have said 'To obtain a coherent physical picture of the microscopic dynamics it is thus required to apply a combination of techniques, and not just a single method, . . .'.

2. Relevant molecular motions

Local molecular packing and motions are believed to be the determining factor for the liquid structure. Long-range motions cannot be influential in defining the density. Distant packing in an amorphous system such as a supercooled liquid cannot be coordinated. Having said this, we can ask for evidence of this presumption.

The kinetics of isothermal volume contraction and expansion of a cured epoxy resin, which is completely amorphous, below its T_g has been followed (Bero and Plazek 1991). Since the volume determines the molecular mobility, contraction following a decrease in temperature is going to be faster than the expansion following an increase to the same temperature since its starting specific volume is larger. This is the reason for the well known asymmetry of approach toward an equilibrium density. To minimize the asymmetry, a series of small temperature jumps of 2.5 °C were utilized in following the contraction and expansion kinetics. Figure 2 shows that the asymmetry is minimal with such temperature changes. This study of physical ageing was different from conventional studies in that each temperature increment was incurred after equilibrium was achieved. The results on the fully cured Epon 1001/DDS are shown in figure 3, where $V(t)$ is the specific volume after the temperature step, and $V(\infty)$ is the equilibrium volume at the final temperature. Since the thermal driving force was virtually the same with each step, simple temperature reduction could be attempted with horizontal timescale shifts. The successful reduction is presented in figure 4. It was assumed that the results were reasonably close to linear behaviour and the more extensive curve obtained from the cooling steps was analysed to obtain a normalized retardation spectrum $L(\tau)$:

$$\int L_0(\tau)\,\mathrm{d}\ln\tau = 1 \tag{1}$$

and then

$$\frac{V(0^+) - V(t)}{V(0^+) - V(\infty)} = \int_{-\infty}^{+\infty} \left(L_0(\tau)\left(1 - \exp\left(-\frac{t}{\tau}\right)\right)\mathrm{d}\ln\tau \right). \tag{2}$$

The $L_0(\tau)$ that was obtained is shown in figure 5 with the retardation spectrum obtained from the shear creep compliance function, $J(t)$. The levels of the short-time behaviour are matched. Three features should be noted. The functionality at short times is the same within experimental uncertainty. The slope of $\log L(\tau)$ at short time indicates that the response is dominated by motions that contribute to Andrade creep (Andrade 1910, 1960, Kennedy 1953, Plazek 1960, Berry 1976, Bero 1994, Bernatz 1999):

$$J_A(t) = J_A + \beta t^{1/3} \tag{3}$$

where t is the time of creep, and J_A and β are characterizing constants.

The positive curvature and the following maximum of the creep compliance $L(\tau)$ indicate the contribution of polymeric molecular modes of motion to the recoverable compliance. Since no positive curvature is seen in the volume contraction $L_0(\tau)$, no polymeric modes are present and no long-range coordinated motions of any kind are detected.

3. Apparent discrepancies

Only local mode molecular motions contribute to changes in the local packing structure of a liquid and the mobility of those modes decreases rapidly with decreasing temperature. At

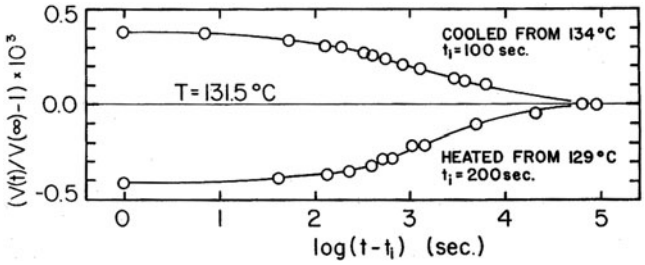

Figure 2. Fractional volume deviation from equilibrium as a function of time at 131.5 °C after cooling from 134 °C and after heating from 129 °C plotted versus the logarithm of the corrected ageing time $t - t_i$ where t_i is the estimated time required for the specimen to reach a uniform temperature.

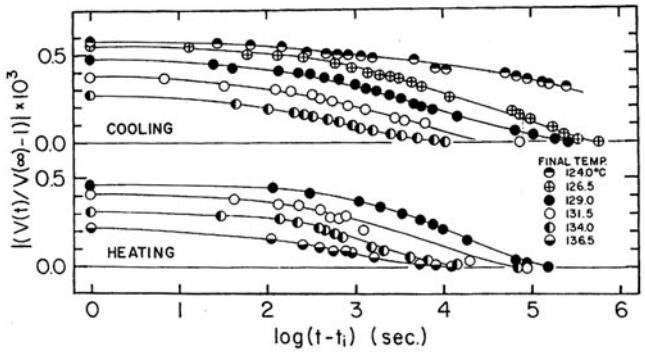

Figure 3. Absolute fractional volume deviation from equilibrium as a function of the logarithm of the corrected ageing time for five temperatures after cooling by increments of 2.5 °C from equilibrium and four temperatures after heating.

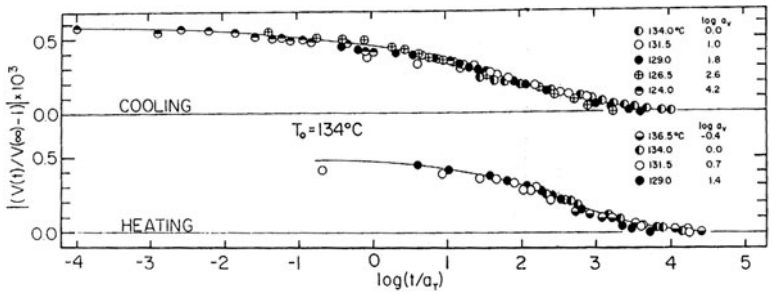

Figure 4. Volume contraction and expansion from figure 3 reduced by timescale shifts to the chosen reference temperature $T_0 = 134$ °C. The time t is the corrected value.

some temperature, because of the diminishing rate of possible molecular rearrangements, the equilibrium liquid structure can no longer be maintained. Below this temperature the liquid is a glass. Therefore the average relaxation time for these motions should be same for all amorphous materials. This expectation was expressed by O'Reilly in his 1987 'Review of structure and mobility in amorphous polymers'. He said 'It was expected that ln τ_g would be constant at T_g within several factors of e(ln $\tau_g \pm t$)'. τ_g is the relaxation time at T_g which he extracted from enthalpy relaxation measurements with the widely used Toole–Narayanaswamy–Moynihan

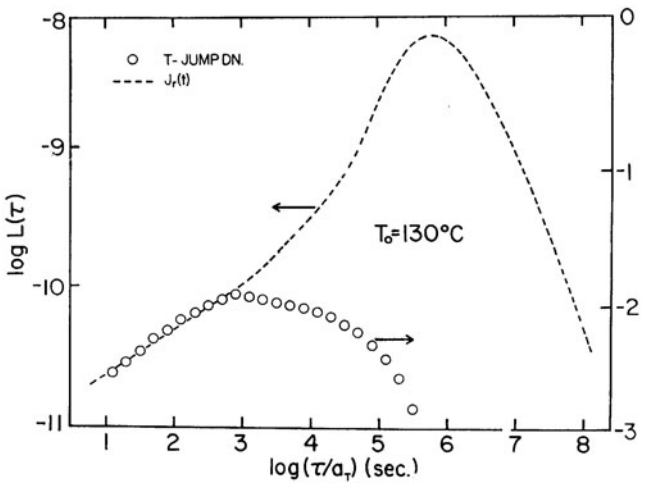

Figure 5. Comparison of retardation spectra for voluminal L_v and shear deformation L_s. In this double-logarithmic plot of the distribution functions of retardation times τ, the ordinate scales have been adjusted to superpose the short-time results.

Table 1. Relaxation times at T_g from O'Reilly (1987). s: syndiotactic; a: atactic; i: isotactic; PAVB: poly(4-vinyl benzo 18-crown).

	T_g (K)	ln τ_g
PS-NBS 706	371	5
PS-38K	368	5–7
PS-321K	373	2
PVC	353	18
PVAc	310	9
	310	6
PMMA-s-H	395	10
PMMA-s-D	394	10
PMMA-a-H	374	10
PMMA-a-D	388	10
PMMA-i-H	326	10
PMMA-i-D	326	10
PC	418	5
As_2Se_3	453	5
B_2O_3	540	8
$(Na_2O)(CaO)(SiO_2)$	740	4
NBS 710	826	5
$(Na_2O)(PbO)(SiO_2)$	706	5
$(Ca(NO_3)_2)_{0.4}(KNO_3)_2$	338	6
5P4E	250	1

model. However, it can be seen in table 1 that ln τ_g was found to vary from 1 to 18, which represents a difference of 7.4 orders of magnitude. The reason for this apparent variation can lie in uncertainties in T_g and/or the model itself. This has not been resolved.

In his third edition of his revered monograph on the '*Viscoelastic Properties of Polymers*' (Ferry 1980) John Ferry presents values for the monomeric friction coefficient ζ_0 at T_g for about three dozen polymers in table 12-III. Examples are shown in table 2 where $\zeta_0(T_g)$ is seen

Table 2. Monomeric friction coefficients at T_g. (Selected values from table 12-III of Ferry (1980), pp 330, 331.)

Polymer	T_g (°C)	$\log \zeta_0$ (dyn s cm^{-1})
Polymethyl methacrylate		
Isotactic	40	6.55
Atactic	106	5.54
Conventional	117	4.97
Polyisobutylene	−68	3.47
Polymethyl acrylate	3	6.24
Polyvinyl acetate	32	4.29
Polystyrene	100	2.06

Table 3. Relative glass temperatures; 20 °C min^{-1} cooling (values as obtained by DSC).

			Superposition temperatures (°C)	
Polymer	T_f (°C)	T_g (°C)	Andrade region figure 10	Softening dispersion figure 11
PS	106	100	100	100
PVAc	43	37	37.6	38
PMA	20	14	10.7	13.1
APP	−5	−9.5	−11.0	−9.5

to vary over $4\frac{1}{2}$ decades. Since $\zeta_0(T_g)$ reflects the molecular mobility at the glass temperature at T_g, we expect all of the values to be the same within experimental uncertainty. In an attempt to investigate the reason for the unexpected variation, as an expedient, measurements were carried out in a DuPont 1090 DSC to obtain comparable results on four polymers: polystyrene, PS; polyvinyl acetate, PVAc; polymethyl acrylate, PMA; and amorphous polypropylene, a-PP. Continuous cooling and heating at 20 °C min^{-1} were utilized, starting from above T_g. Glass temperatures, T_g, were deduced from the behaviour in cooling and fictive temperatures, T_f, were estimated from the heating curves. If negligible ageing occurs during heating, the temperature at which the equilibrium enthalpy is crossed is T_f. The absolute readings were recognized to be incorrect, as evidenced by the fact that the T_f-readings were higher than the T_g-readings, which is an impossibility. In fact, all T_fs for a given rate of heating are lower than T_g determined at an equal rate of cooling.

Creep and recovery measurements were also carried out on the same polymers, and retardation spectra, $L(\log \tau)$, were obtained from the recoverable compliance curves, $J_r(t)$. Using the polystyrene $L(\log \tau)$ at 100 °C as a reference, the temperatures at which the $L(\log \tau)$ of the other polymers superposed in both the local mode motion (Andrade creep) and the Rouse mode (softening dispersion) regions were determined and these are shown in figures 5 and 6 respectively. The results are presented in table 3. At the time at which these comparisons were made, it was not clear which was the proper comparison. However, the temperature dependences are so great that the results are within two degrees of one another. The estimated T_gs are within 2 °C of the superposition temperature averages. It is clear that the literature values of T_g for PMA and PVAC are low by 11 and 5 °C respectively. These differences are responsible for their apparently larger $\log \zeta_0(T_g)$ values. An 11 °C temperature difference easily accounts for a difference of four orders in magnitude in mobility. Likewise a 5 °C discrepancy causes a hundredfold difference.

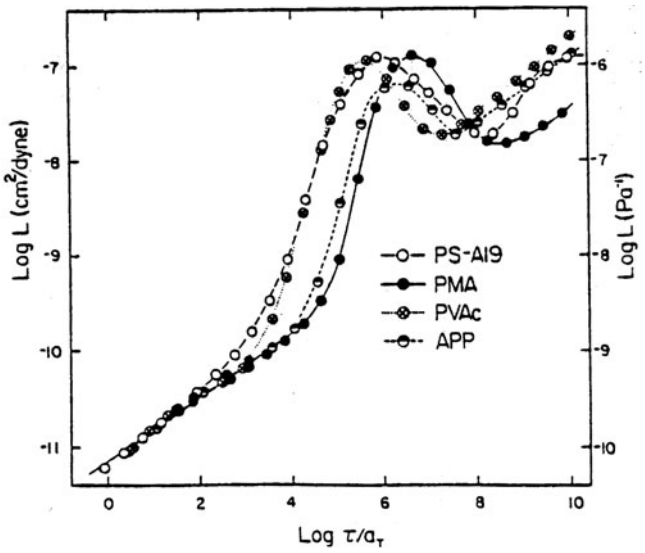

Figure 6. Softening portions of $L(\tau)$ for polystyrene (PS), polymethyl acrylate (PMA), polyvinyl acetate (PVAc), and amorphous polypropylene (APP) shown with Andrade regions superposed. The polystyrene L is the reference curve at its position at $T_g = 100\,^{\circ}\mathrm{C}$. Reference temperatures for the other polymers are presented in table 3.

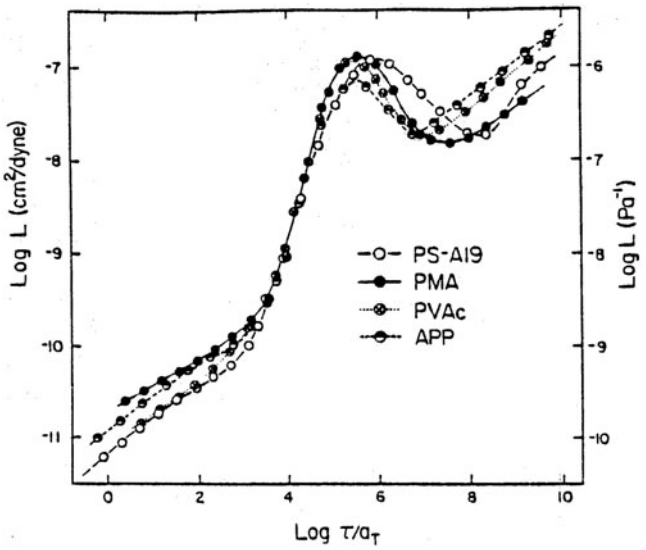

Figure 7. Short-time portions of the retardation spectra as displayed in figure 6 with the ascending portions of the symmetrical peak superposed. The polystyrene $L(\tau)$ is the reference curve. Reference temperatures are listed in table 3.

Before proposing a path to relatively precise T_gs, we wish to examine the systematic variation of the viscoelastic functions with the molecular structure. Because of the additivity of strains arising from different molecular mechanisms (Plazek 1992, Plazek and Echeverria 2000), it should be noted that the clearest picture is seen in the development of $L(\log \tau)$ with changes in molecular weight. Effects of branching and molecular weight distribution are not

considered here. The most complicated viscoelastic response is exhibited by high-molecular-weight polymers with entangled linear molecular chains. The data shown were obtained for a narrow-distribution polystyrene with a molecular weight of 3.8×10^6. The qualitative behaviours of the most frequently examined viscoelastic functions are shown logarithmically in figure 8 as functions of time (t) and frequency:

(a) the shear creep and recoverable (dashed line) compliance $J(t)$;
(b) the stress relaxation modulus $G(t)$;
(c) the dynamic storage (J') and loss (J'') compliances;
(d) the dynamic storage (G') and loss (G'') moduli;
(e) the loss tangent $\tan\delta = J''/J' = G''/G'$;
(f) the real component of the dynamic viscosity (η') and the imaginary component (η'');
(g) the retardation function $L(\tau)$; and
(h) the relaxation spectrum $H(\tau)$.

Rubbery entanglement plateaus are seen in (a)–(d). Two maxima are seen in the spectra. The behaviour of a low-molecular-weight polystyrene ($M = 1.64 \times 10^4$) is similarly depicted in figure 9. No rubbery plateau is present and the spectra have only a single maximum. Even simpler viscoelastic functions describe the behaviour of a non-polymeric glass-former dehydroabietic acid as shown in figure 10.

By examining the different regions of $L(\log\tau)$ for a high-molecular-weight polystyrene ($M = 3.8 \times 10^6$) we can see clearly how the behaviour evolves with decreasing molecular chain length. This is shown in figure 11 where four regions of response are visible at the longest retardation times; a symmetrical peak, centred at $\log(\tau) = 16$, reflects the long-range coordinated motions involving entangling and disentangling in the approach to the steady-state recoverable compliance J_s.

In the timescale region between values of $\log\tau$ of 10 and 13 an Andrade creep mechanism dominates the response which probably reflects the attrition of short segments in the entanglement network. This segment is linear with a slope of $1/3$. At still shorter times, another symmetrical peak is seen, centred at $\log\tau = 7$. This represents contributions to the compliance in the higher portion of the softening dispersion where Rouse and sub-Rouse modes of motion operate. As the molecular weight is decreased, the length of the rubber plateau, which is the distance between the two peaks, diminishes with the 3.4 power of the molecular weight. The plateau reaches zero length at M_c, the critical molecular weight where the molecular weight dependence of the viscosity decreases from $M^{3.4}$ to $M^{1.0}$ (at constant L_0) (Plazek 1992).

Finally, at the shortest times shown, between $\log\tau = -1$ and 4, glassy Andrade creep dominates. $\log L(\tau)$ is a straight line with a slope of $1/3$. This region is dominated by the local mode motions, which are involved in determining the local liquid or liquid-like structure. These are the same motions that are involved in determining T_g.

It is important to note that near T_g we see the strongest temperature dependences of kinetic processes. Therefore large changes in such variables can reflect small temperature changes. This temperature dependence is still believed by some, including the authors, to be intrinsically a relative free volume dependence. Kinetic variables like the weight average terminal relaxation time $\tau_t = \eta J_s$, where η is the shear viscosity coefficient, change with time in physical ageing experiments under isothermal and isobaric conditions. Since the temperature is constant in such experiments, the changes cannot be attributed to the presence of a change in thermal kinetic energy. Many critics of the influence of the relative free volume refer to volume changes without acknowledging possible changes of occupied volume v_o which is a vital contribution to the relative free volume. $\Phi = (v - v_o)/v_o$, where v is the specific volume.

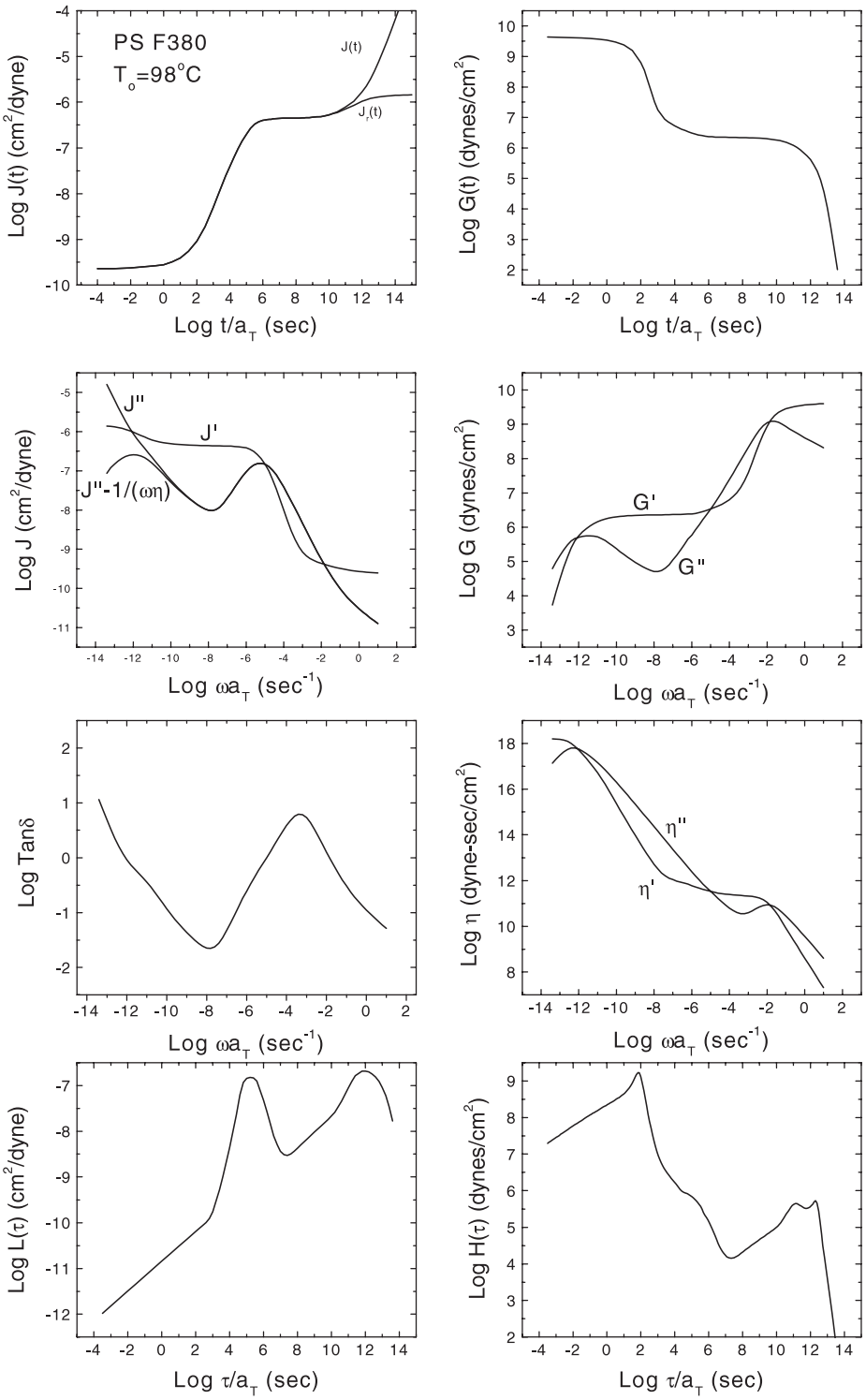

Figure 8. Viscoelastic functions of a high-molecular-weight entangled polymer (polystyrene, $M = 3.8 \times 10^6$).

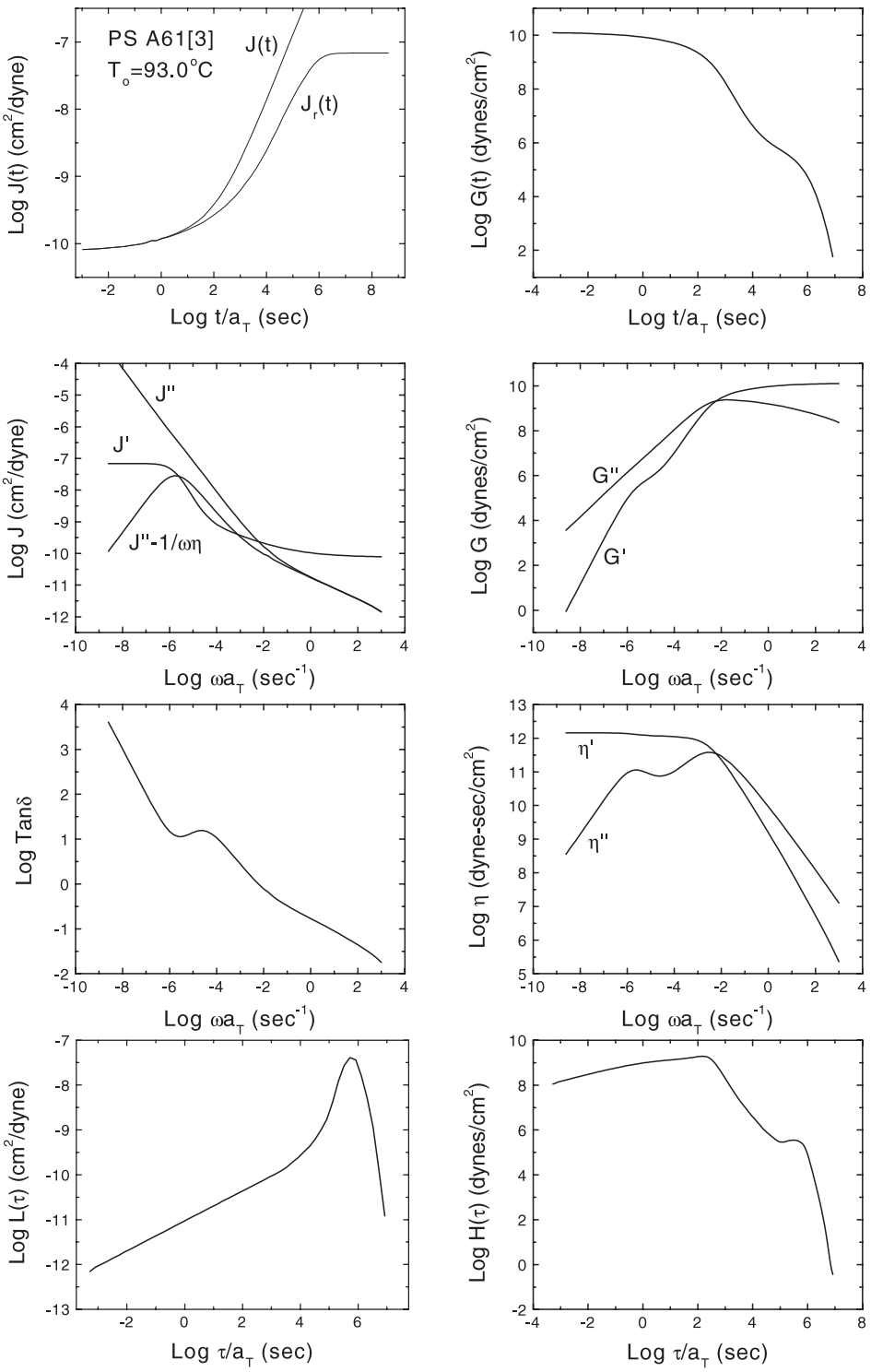

Figure 9. Viscoelastic functions of a low-molecular-weight polymer (polystyrene, $M = 1.64 \times 10^4$).

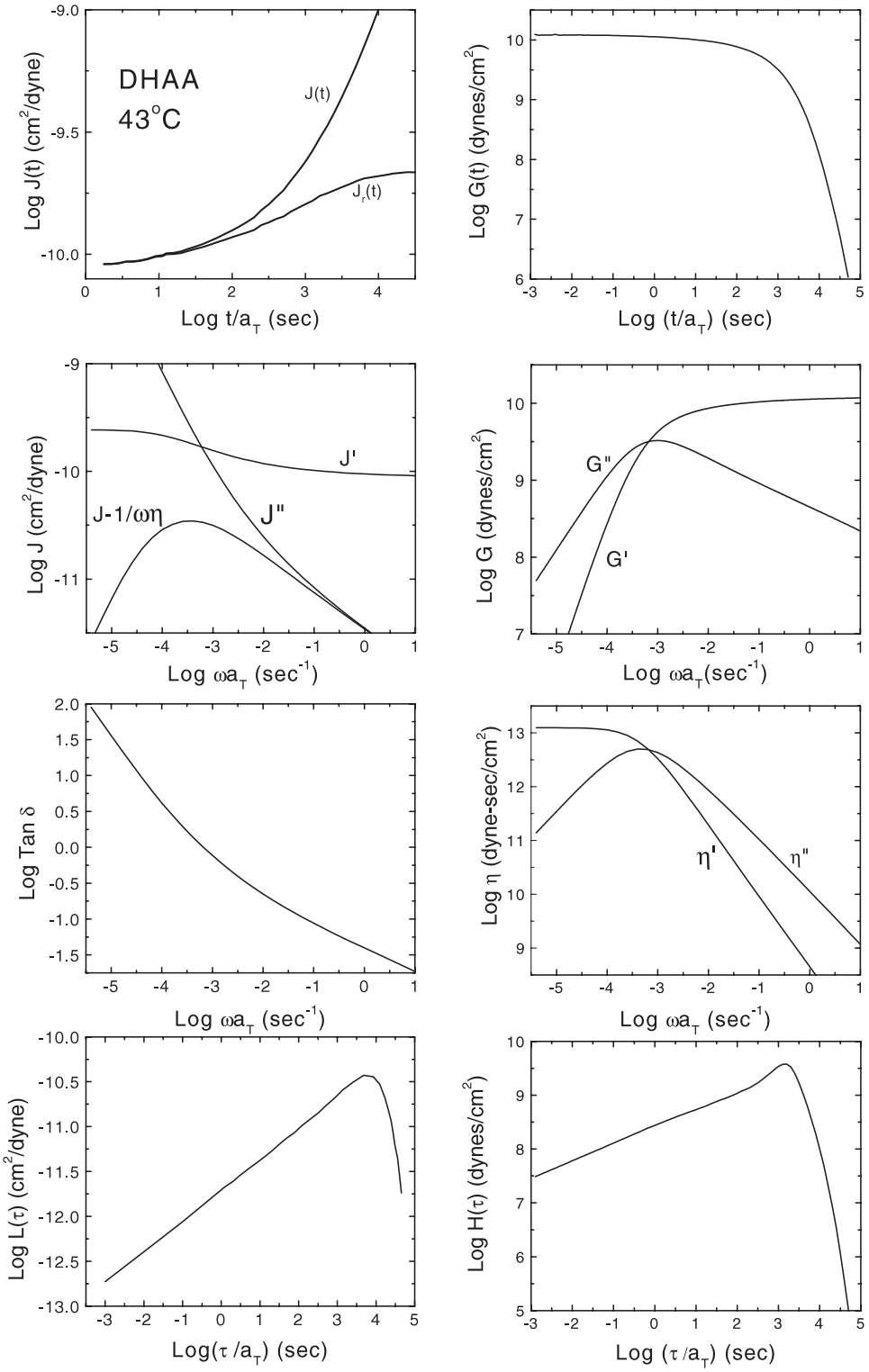

Figure 10. Viscoelastic functions of a non-polymeric glass-former (dehydroabietic acid).

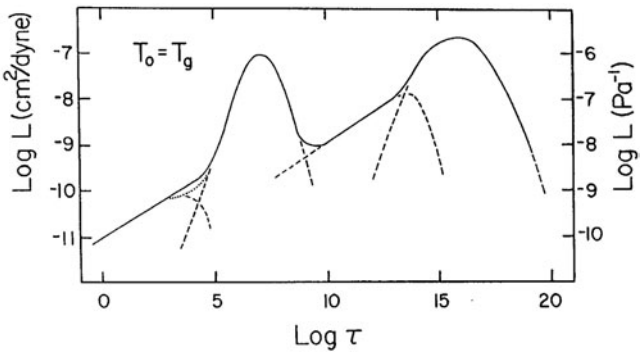

Figure 11. The retardation spectrum of a narrow-molecular-weight-distribution polystyrene (mol wt $= 3.8 \times 10^6$) at $T_g = 98\,^{\circ}$C.

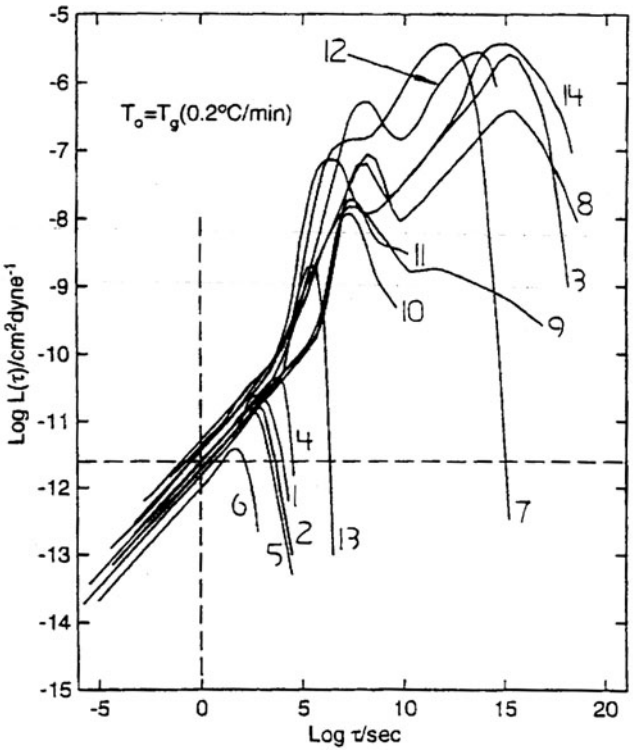

Figure 12. Comparison of the retardation spectra at $T_0 = T_g$ ($0.2\,^{\circ}$C min^{-1}) for: (1) 6 PE; (2) Aroclor 1248; (3) polypropylene; (4) TCP; (5) OTP; (6) $Tl_2SeAs_2Te_3$; (7) PS Dylene 8; (8) PIB; (9) Viton 10 A; (10) Epon 1004/DDS; (11) Epon 1007/DDS; (12) PB/Aroclor 1248 solution; (13) Se; (14) PVAc.

4. Universal behaviour at T_g

Since the mobility of the local mode motions determines T_g, a kinetic characterizing variable, such as the Andrade coefficient β, which is determined by these motions, can be associated with T_g. If we examine the glassy Andrade regions of the retardation spectra for many amorphous

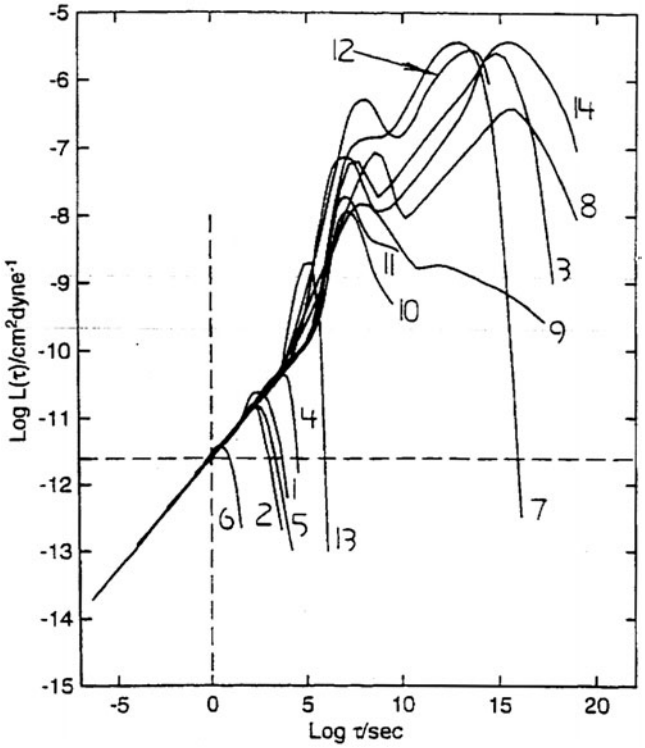

Figure 13. Superposition of the retardation spectra at short times for the glass-formers of figure 12.

materials at their respective T_gs, we find that they are all close to one another, as seen in figure 12. Fourteen amorphous materials including organic and inorganic polymers and non-polymers are represented. They are identified in table 4 of (Bero 1994).

In producing figure 12, the best T_gs that were available for a cooling rate $Q = 0.2\,^{\circ}\mathrm{C\ min}^{-1}$ were used to fix the timescale. The variability relative to the average position is about one decade on the timescale. Tricresyl phosphate (TCP) was chosen as the reference material; i.e. the position of its $\log L(\tau)$ was assumed to be correct for its T_g ($0.2\,^{\circ}\mathrm{C\ min}^{-1}$ cooling). The T_gs of the other glass-formers were adjusted to match the position of the glassy Andrade region to that of the TCP. With the exception of a chalcogenide alloy of thallium, selenium, arsenic, and tellurium, the required changes of the T_gs were about $2\,^{\circ}\mathrm{C}$ or less. The T_g-adjustments are listed in table 4 of (Bero 1994). Since glass temperatures are often in doubt by more than several degrees, it is felt that the Andrade line seen in figure 13 represents all of the materials within experimental uncertainty and therefore the common curve can be used to determine relative T_gs with a precision that is not achievable by any other means. The T_g of the quaternary alloy is in doubt and should be checked.

5. Determination of T_g from the compliance functions

From the common line in the retardation functions shown at T_g in figure 13, the Andrade β-coefficient can be calculated. Smith (1959) showed that when Andrade creep is observed,

$$L(\tau) = 0.246\beta\tau^{1/3}.$$

Therefore since, at T_g, $L(\tau) = 2.24 \times 10^{-12}$, we have, at $\tau = 1$ s,

$$\beta = 9.11 \times 10^{-12}\ (\mathrm{cm}^2\ \mathrm{dyn}^{-1}\ \mathrm{s}^{-1/3})$$

or

$$\beta = 9.11 \times 10^{-11}\ (\mathrm{m}^2\ \mathrm{N}^{-1}\ \mathrm{s}^{-1/3}),$$

and one simply has to determine β as a function of temperature to find out where β has this value in order to determine T_g. The T_g defining β can be obtained from dynamic mechanical properties as well as from the recoverable creep compliance $J_r(t)$, since we showed (Plazek 1960) that

$$J'(\omega) = J_A + 0.773\beta\omega^{-1/3}$$

and

$$J''(\omega) = 0.446\beta\omega^{-1/3}$$

when $J'(\omega)$ and $J''(\omega)$ are the storage and loss components of the complex dynamic compliance:

$$J^*(\omega) = J'(\omega) - \mathrm{i}J''(\omega)$$

and β is the same Andrade coefficient as seen in $J_r(t)$.

Acknowledgments

This work was supported by the National Science Foundation (USA) under grant No DMR-9531372. We also wish to acknowledge the assistance given by Stephen J Orbon with some of the calculations.

References

Andrade E N D A C 1910 *Proc. R. Soc.* A **84** 1
Andrade E N D A C 1960 *Proc. R. Soc.* A **254** 291
Bernatz K M 1999 *PhD Thesis* University of Pittsburgh, PA
Bero C A 1994 *PhD Thesis* University of Pittsburgh, PA
Bero C A and Plazek D J 1991 *J. Polym. Sci.* **29** 39
Berry G C 1976 *J. Polym. Sci.* **14** 451
Bohmer R, Diezemann G, Hinze G and Rossler E 2001 *Prog. Nucl. Magn. Reson. Spectrosc.* 191
DeBolt M A, Eastead A J, Macedo P B and Moynihan C T 1976 *J. Am. Ceram. Soc.* **59** 12
Ferry J D 1980 *Viscoelastic Properties of Polymers* 3rd edn (New York: Wiley)
Greiner R and Schwarzl F R 1984 *Rheol. Acta* **23** 378
Kennedy A J 1953 *J. Mech. Phys. Solids* **1** 172
Kovacs A J 1964 *Adv. Polym. Sci.* **3** 394–507
LeMay J D, Swetlin B J and Kelley F N 1984 *Characterization of Highly Cross-Linked Polymers (Am. Chem. Soc. Symp. Ser. 243)* ed S S Labana and R a Dickie (Washington, DC: American Chemical Society)
O'Reilly J M 1987 *CRC Crit. Rev. Solid State Mater. Sci.* **13** 259
Plazek D J 1960 *J. Colloid Sci.* **15** 50
Plazek D J 1992 *J. Rheol.* **36** 1671
Plazek D J and Echeverria I 2000 *J. Rheol.* **44** 831
Plazek D J and Frund Z N Jr 1990 *J. Polym. Sci.* **28** 431
Plazek D J and Ngai K L 1996 *Physical Properties of Polymers Handbook* ed J E Mark (Woodbury, NY: AIP) ch 12 pp 139–60
Plazek D J, Rosner M J and Plazek D L 1988 *J. Polym. Sci.* **26** 473
Richardson M J and Savill N G 1975 *Polymer* **16** 753
Richardson M J and Savill N G 1977 *Polymer* **18** 3
Sasabe H and Moynihan C T 1978 *J. Polym. Sci.* **16** 1447
Smith T L 1959 personal communication